Paper available at: https://www.tandfonline.com/doi/full/10.1080/13632469.2018.1463879

Seismic performance of historical buildings based on Discrete Element Method: An adobe church

Nuno Mendes[a], Sara Zanotti[b], and José V. Lemos[c]

[a]ISISE, University of Minho, Guimarães, Portugal; [b]University of Minho, Guimaraes, Portugal; [c]Department of Concrete Dams, LNEC - National Laboratory for Civil Engineering, Lisboa, Portugal

Abstract

This paper presents the main concepts and the application of the Discrete Element Method for evaluating the seismic performance of historical buildings. Furthermore, the out-of-plane behavior of an adobe church with thick walls, in which the morphology of the cross-section can have an influence on the response, was evaluated by the Discrete Element Method. The performance of rigid and deformable blocks models was compared, and the sensitivity of the numerical model to the variation of critical parameters was investigated. The results allowed the identification of the most vulnerable elements and a proposal of recommendations for reducing the seismic vulnerability.

Keywords: Adobe; Church; Earthquake; DEM, Out-of-plane behavior, Pushover analysis.

1. Introduction

Historical buildings are associated with cultural identity and should be preserved. In general, these types of buildings are vulnerable to seismic action, which can cause major and irrecoverable losses for countries and societies. The seismic assessment of historical buildings is complex and depends on several parameters [Lourenço et al., 2011], in which their out-of-plane behavior is still a challenge [Mendes et al., 2017].

In what concerns the material behavior, historical buildings were built using earth, wood, and regular or irregular stone masonry. These types of materials present complex properties and are difficult to model [Roca et al., 2010]. Three main modeling approaches for masonry were proposed by Lourenço [2002], namely detailed micro-modeling, simplified micro-modeling and macro-modeling [e.g. Chácara et al., 2017].

Several types of analysis have been used for evaluating the seismic behavior of masonry structures. Limit analysis, first adopted by Heyman [1969] for the assessment of masonry arches, allows the evaluation of the load capacity of masonry structures based on two approaches, namely the static approach (thrust line) and the kinematic approach (mechanism with macroblocks). Pushover analysis has also been widely adopted for evaluating the seismic performance of masonry buildings [e.g. Peña et al., 2010]. Nonlinear dynamic analysis with time integration requires a high computational effort and has been used less often [e.g. Mendes and Lourenço, 2014].

Finally, different types of methods for modeling masonry structures are available, such as the methods based on an equivalent frame with 1D elements [e.g. Magenes and Fontana, 1998], methods in which the structural elements are modeled by 2D macro-elements [e.g. Lagomarsino et al., 2012], the Finite Element Method (FEM) [e.g. Mendes and Lourenço, 2010] and the Discrete Element Method (DEM) [e.g. Azevedo et al., 2000].

The DEM is capable of simulating the behavior of complex masonry structures, including the modeling of the real unit arrangement. Thus, this paper presents the general concepts of DEM and their application for evaluating the seismic performance of historical buildings. Furthermore, the seismic performance of the Kuño Tambo church (Peru), an adobe church with thick walls, was assessed using the DEM. Two DEM models taking into account the morphology of the cross-section were prepared, aiming at evaluating the

out-of-plane behavior of the longitudinal wall of the nave and the out-of-plane behavior of the main façade.

2. Discrete element models for historical buildings

2.1. General concepts of DEM

The discrete element method has gained acceptance in many fields dealing with discontinuous media or blocky systems. From its early stages in rock mechanics, this approach has been mostly intended to study failure processes governed by joints and interfaces, often involving large relative movements between system components. This objective underlies the choice of an explicit time-stepping algorithm, which allows easy updating of the system geometry and contact conditions. The analysis of quasi-static problems relies on the same algorithm as in classical dynamic relaxation, employing artificial damping and scaling methods for efficient solution. These features make the method, for which diverse formulations and implementations are available, a very appropriate tool for masonry structures [Lemos, 2007].

The solution procedure adopted by DEM is particularly effective in the simulation of the progressive development of collapse mechanisms, as the block movements induced by separation and sliding along the joints can be closely followed, up to structural failure. It is possible to perform either a pushover analysis, by means of a sequence of static runs with increasing loads until the maximum load is attained, or a full dynamic analysis in the time domain, to evaluate the level of damage caused by an earthquake recorded with a given intensity.

The first choice to be made when building a DEM representation is between rigid and deformable blocks, the latter being discretized into an internal FE mesh, sometimes referred to as FDEM. The results presented in the present paper confirm previous studies showing that rigid block models provide a good performance for a fairly wide range of

masonry problems. In DEM codes, the interaction between blocks is typically based on the point contact assumption, in which the normal and shear stress at a contact are a function of the relative displacement at the contact point [Lemos, 2007]. This simplification, however, still allows proper accuracy if a sufficient number of contact points is used. For rigid blocks, it may require subdividing the polygonal faces into a finer mesh of triangles, to create more contact points at the extra nodes. The code 3DEC [Itasca, 2015], employed in this paper, displays these typical features of DEM codes, the key issues raised by its application to masonry being discussed in Lemos [2016].

2.2. Applications of DEM to complex structures

The early applications of DEM models to masonry involved simple structures, such as arches or drum columns [e.g. Psycharis et al., 2003]. These structural components, mostly involving stone masonry, are still the main field for block models. More elaborate cases have progressively been analyzed, for example, historical masonry vaults [e.g. McInerney and DeJong, 2015].

The increase of computer processing power has enabled larger and more complex structures to be approached. For example, in the study of classical monuments, instead of single columns, the representation of larger structures has been attempted. Psycharis et al. [2011] studied the behavior of the Parthenon walls with a rigid block model, examining, in particular, the effects of different seismic motions. Young et al. [2015] developed a model of the ancient temple of Nemea to investigate if an earthquake was a plausible cause of collapse.

However, it is obviously impossible to include each individual unit of a complex structure. A numerical model is always a simplified representation of reality, and the issue is how much detail is required to achieve realistic results. Often, a larger joint spacing or block size may be used, as long as the global arrangement is respected, and there are

sufficient joints and blocks to allow the potential failure modes to develop. A shake table test of a 1-story stone masonry house [Mendes et al., 2017] provided some material for this discussion. A 3DEC rigid block model was employed in a dynamic simulation of the test [Lemos and Costa, 2017]. The numerical model did not attempt to reproduce the exact stone block shapes, only the general joint pattern and the average dimensions of the units. Nevertheless, the model provided a fairly good representation of the observed deformation and near collapse modes. A pushover analysis carried out with the same model also achieved a good match of the observed failure pattern, even if the required acceleration was conservatively underestimated, as would be expected. Catki et al. [2016] analyzed the shake table test of a mosque model, and were able to obtain the observed magnitude of peak responses, as well as the natural frequency drop due to progressive joint opening and loss of contacts.

The representation of irregular units is another important issue in the study of traditional structures. De Felice [2011] was able to create a model with irregular stone shapes in 2D analysis of 3-leaf wall sections. For the 3D case, the run times would still be prohibitive, except for small local models. There are also simplified approaches to include some amount of randomness in the numerical geometry, such as the use of Voronoi polyhedra, as was done for the base course in the present church model.

3. Kuño Tambo church

3.1. Historical context

The Kuño Tambo church, also known as the Church of Santiago Apóstol, is an adobe church of a rural village with about 500 inhabitants located in the province of Acomayo southeast of the city of Cusco (Peru). The church has been used by the community since its construction in the seventeenth century, and is an important gathering and religious place for the community members. The interest demonstrated by the community in the

rehabilitation of the church led the Cusco regional office of the Ministry of Culture of Peru to begin the process to nominate the entire town, including the Kuño Tambo church, as a national monument due to its originality, authenticity and preservation of earthen buildings and construction techniques [Cancino et al., 2012].

The first reference to the village of Kuño Tambo is found in a document of 1577, which refers to the four *suyos* (regions) of Cusco; *Cocno*, the earliest name of Kuño Tambo, was listed as one of the villages belonging to the *suyo Condesuyo* [Cancino et al., 2012]. It is a typical village constructed by the Spanish Viceroyalty aiming at organizing the indigenous culture. The Kuño Tambo village (FIGURE 1) was constructed under the governance of Viceroy Francisco de Toledo. During the Toledo Viceroyalty, more than 1000 Indian villages called *reducciones* were constructed. The *Primer Concilio Provincial Limense* (First Council of the Archdiocese of Lima) stated that churches should be built in each *reduccion* [Cancino et al., 2012].

Juan de Matienzo, who in 1567 wrote "Government of Peru", focused on the physical layout of the *reducciones*, sketching a model plan. The plan specified a village of five hundred households, organized in square blocks which surrounded a plaza and a church. Matienzo specified that the church should be built in one block located in front of the plaza, as in Kuño Tambo village (FIGURE 1). The other square blocks around the plaza were reserved for a municipal hospital, the house of the *Corregidor de indios* (the mayor of the village), a jail and an inn for travelling Spaniards. The native people lived in blocks far from the plaza [Mumford, 2012].

According to the documents of the Acomayo Parish Archive, the Kuño Tambo church, named as *el Templo de Santiago Apòstol de Cunotambo*, was built in 1681. Before that, the village was included in the parish of San Juan de Quihuares. In general, churches were built with the façade directly facing the main plaza. However, Kuño Tambo Church has

a different orientation. Probably, it was built over an existing temple, which did not have any relationship to the new plaza constructed after the Toledo reform. It is noted that the Third Constitution indicated that old temples should be destroyed. However, if the location was appropriate, the new church should be built in the same place [Cancino et al., 2012].

FIGURE 1 Aerial view of Kuño Tambo village (Peru) and location of the church [Cancino et al., 2012].

3.2. Description of the church

The Kuño Tambo church is a one-story building composed by the nave, presbytery with altar, baptistery, sacristy and choir loft (FIGURE 2a). Furthermore, it has a bell tower not structurally connected to the building (FIGURE 1). The walls were built with adobe bricks on a base course (FIGURE 2b). The roof was constructed with timber elements, based on the *par y nudillo* method. The *par y nudillo* is a traditional method that consists of two rafters with a diameter of 0.20 m, joined through a collar tie (FIGURE 2c). The church was constructed on a natural rock outcrop. Compacted clay fill layers were used

to level the site. Thus, the foundation sits directly on the natural rock or the compacted clay fill. Currently, the church has two buttresses at the east wall of the nave. Two buttresses that existed at the west wall of the nave have collapsed. In addition, the church has buttresses at the corners that correspond to extensions of the walls (FIGURE 2a).

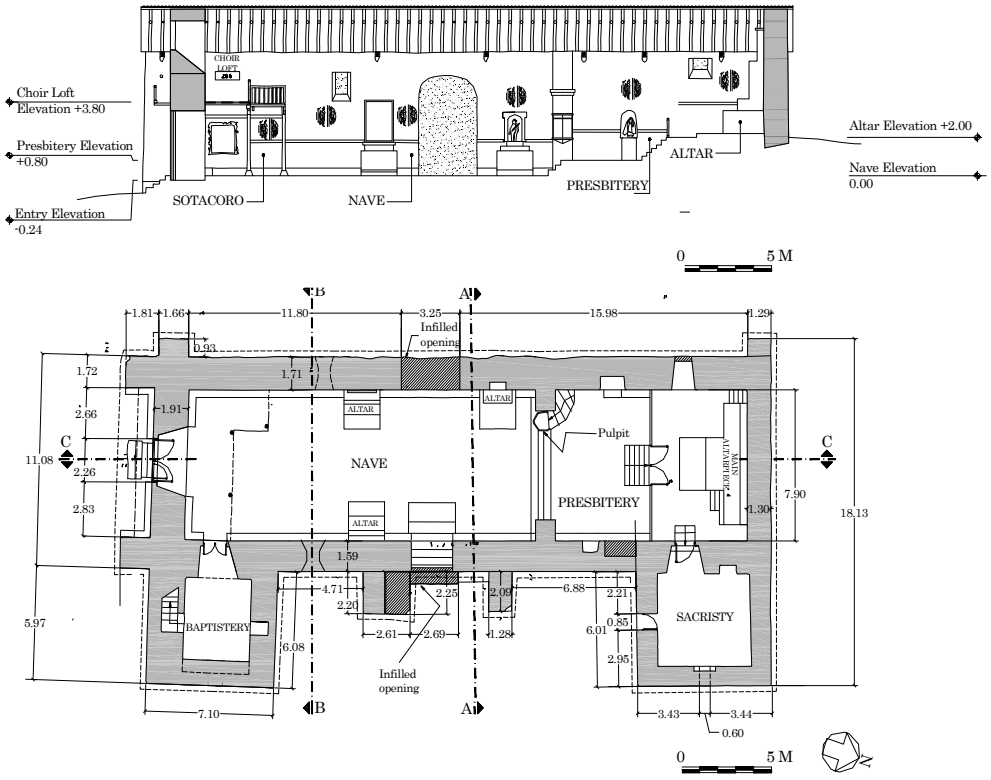

(a)

(b)

(c)

FIGURE 2 Kuño Tambo church: (a) Plan and longitudinal section; (b) Main façade; (c) Roof of the nave [Cancino et al., 2012]. (Dimensions in meters)

The walls are of load-bearing mud brick with English bond pattern and mud mortar. The typical brick dimensions are 0.70 m long x 0.35 m wide x 0.2 m high. The average thickness of the joints is 15 mm. The base course is constituted by rubble stone masonry

and mud mortar, in which some stone units exceed 0.64 m in width and the thickness of the mud mortar ranges from 20 to 60 mm. The base course varies in height following the natural slope of the site (1.20 to 1.50 m). The walls present a plaster finish at both the interior and exterior faces. The interior plaster consists of a layer of mud and straw with 20–30 mm of thickness [Cancino et al., 2012].

The thickness of the lateral walls of the main nave varies between 1.60 m and 1.90 m, with a maximum height of 6.60 m (measured from the visible top of the rubble stone masonry base course). The main façade, located south, and the north wall have a thickness of 1.90 m and 1.30 m, respectively. The height of the façade at the gable end is 8.70 m. In general, the walls are well connected to each other by the overlapping of mud bricks, with the exception of the baptistery, which was constructed adjacent to the eastern wall of the main nave (FIGURE 2a). However, the southern and the northern walls are not well connected to the lateral main nave walls. Regarding the buttresses placed along the east wall of the nave, all are connected to the nave walls with overlapping bricks.

3.3. Main interventions

Although all the buildings of Kuño Tambo village were built at the same time, the church has been subjected to several alterations. The repointing technique was applied in some parts of the structure, in order to consolidate the portion of the walls affected by wind erosion. Currently, the bricks units are more deteriorated than the mortar joints. The walls were subjected to several alterations, mainly in the window and door openings, some of which were infilled with bricks. The two lateral doors located at the center of the longitudinal walls of the nave are now infilled with adobe masonry without connection to the original walls (FIGURE 2a). The two earthen buttresses at the west lateral wall collapsed and only the presence of a rubble stone masonry course remains. At the east

lateral wall, the buttresses were strengthened by adding new adjacent buttresses without structural connection to the existing walls. Currently, only one of the strengthening buttresses remains (FIGURE 2a).

In the interior of the church, it is possible to observe two mud brick piers (FIGURE 3), which are probably the remains of a *quincha* (wattle and daub) arch, constructed in order to separate the nave from the presbytery. A similar *quincha* arch without damage is observed in the church of the nearby Rondòcan village, which presents a design similar to Kuño Tambo church. The causes of the collapse or of the dismantling of the arch are not documented. However, the pier exhibits cracking, probably related to the out-of-plane movement of the west wall, which denotes an outward displacement. The current roof was reconstructed after the collapse of the *quincha* arch. The previous roof probably had a shape compatible with the arch and it would be taller than the existing roof. When the roof was replaced, vegetal ropes were used to connect rafters, and iron nails to connect the rafters with the collar ties, instead of the original leather straps. In addition, three wooden keys were installed at the south ends of the east and west walls, aiming at improving the connection between the rafters and mud brick walls (FIGURE 4). A wood key was also installed at the north wall of the baptistery [Cancino et al., 2012; Ferreira and D' Ayala, 2012].

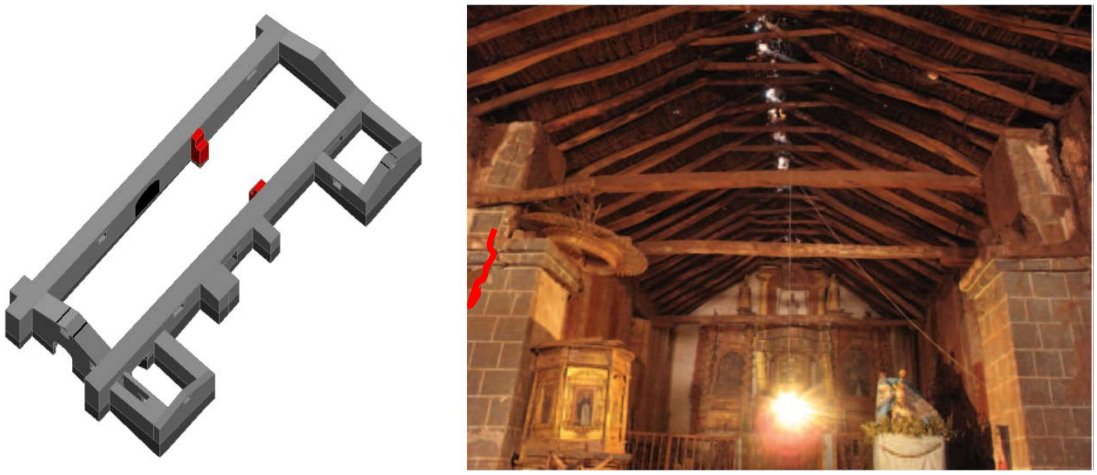

FIGURE 3 Remains of the *quincha* arch [Karanikoloudis and Lourenço, 2015].

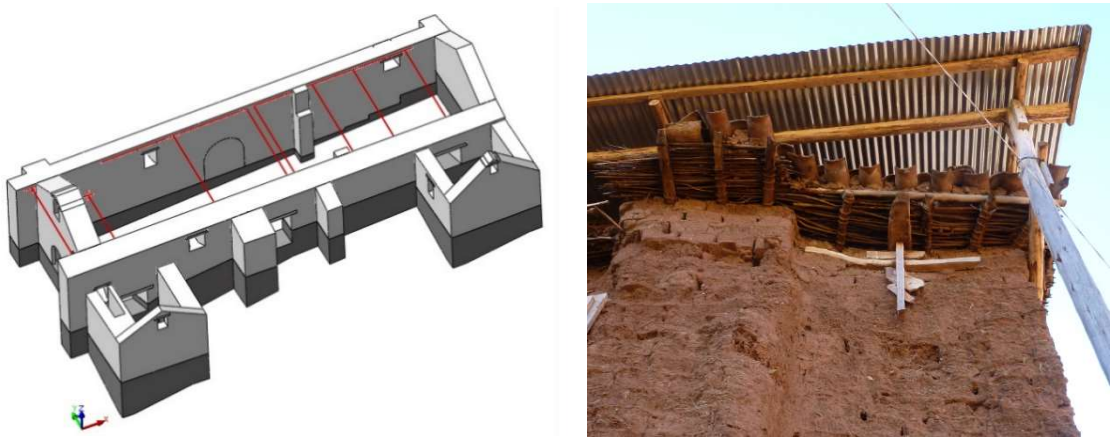

FIGURE 4 Locations of tie beams and detail of the wood key at the southwest corner [Karanikoloudis and Lourenço, 2015].

3.4. Damage survey

The damage survey (FIGURE 5), carried out by University of Minho (Portugal), showed that the main façade (south) presents vertical cracks at the corners, which are visible from both the interior and exterior faces. The west and east longitudinal walls also present cracks and out-of-plane deformations. The baptistery has a vertical crack at each transversal wall and several cracks at the southeast corner. These cracks can be associated with the damage caused by earthquakes in the past and/or settlements at the base course. The walls also present other types of damage, such as efflorescences, deterioration of mortar of the joints and losses of material, mainly at the base course (FIGURE 5).

FIGURE 5 Damage on the masonry walls.

In general, the roof is in poor condition, as some connections between the rafters and the collar ties are not efficient, and some of the structural elements present deformations. The covering of the roof is also in poor condition and allows water infiltrations, causing not only the erosion of the adobe bricks at the top of the walls, but even the detachment and loss of the interior plaster. Currently, the roof is protected by a provisional structure (FIGURE 2b).

3.5. Dynamic identification tests

The dynamic identification tests performed by University of Minho aimed at estimating the dynamic properties of the Kuño Tambo church, namely natural frequencies and mode shapes [Greco et al, 2015]. The ambient vibration tests were carried out using piezoelectric accelerometers (10 V/g) fixed at the top of the walls.

The dynamic identification tests allowed the estimation of four modes with frequency ranging from 1.59 Hz to 2.99 Hz (FIGURE 6). The first mode (1.59 Hz) corresponds to the first global transversal mode of the church. The longitudinal walls present single curvature and are out-of-phase. Furthermore, the southwest corner presents high amplitudes, which can be associated with the existing damage. The second mode (2.15 Hz) corresponds to a mode in the longitudinal direction, in which the out-of-plane vibration of the façades is highlighted (first local mode of the façades). The third mode (2.68 Hz) is a combined mode. Finally, the fourth mode (2.99 Hz) corresponds to the second local mode of the main façade.

4. Out-of-plane behavior of the longitudinal wall

The longitudinal west wall of the nave does not have buttresses that would allow the reduction of out-of-plane displacements. Besides, the Kuño Tambo church has thick walls composed by several units along the transversal direction of the wall. Therefore, it was

important to assess the out-of-plane behavior of the west longitudinal wall of the church, taking into account the morphology of the cross-section. FIGURE 7 presents the geometry of the adopted cross-section wall with unitary width. The adobe units are about 0.70x0.35x0.20 m and the thickness of the joints is equal to 15 mm. The maximum dimension considered for the stone units of the base course of the wall was 0.70 m. A constant value of 30 mm was adopted for the thickness of the joints of the base course. It is noted that the total thickness, including the plaster, of the wall is 1.71 m. However, the plaster was not considered, resulting in a wall thickness of 1.64 m.

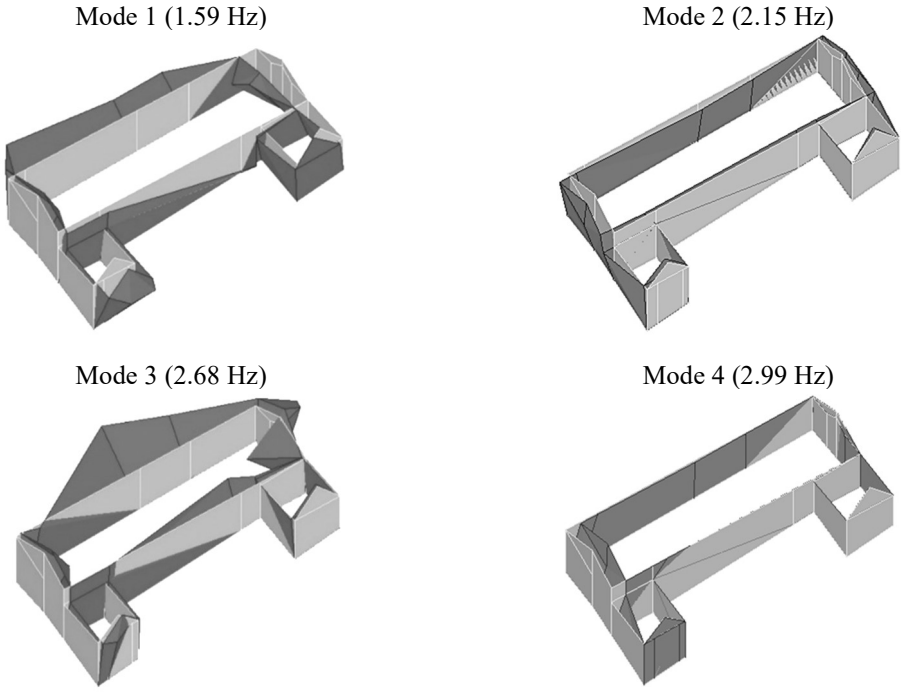

FIGURE 6 Natural frequencies and mode shapes estimated through dynamic identification tests [Greco et al., 2015].

The numerical model was prepared in the 3DEC software [Itasca, 2015], which is based on the Discrete Element Method (DEM). In the DEM, the masonry units are modeled through blocks that interact with each other by contact interfaces. In general, the masonry units are expanded to include the thickness of the joints. As a consequence of this procedure, the adobe units were modeled by blocks of 0.715x0.315x0.215 m and the joints have zero thickness. The rubble masonry of the base course was simulated by

Voronoi polygons, taking as reference the real morphology of the masonry. A Voronoi diagram is, from a mathematical point of view, a partitioning of a plan into regions based on the distance to points in a specific subset of the plan. Given a set of points, it is possible to construct a Voronoi diagram drawing equidistant lines between the points considered, in order to define the regions of points closer to each one of the original points. This data set of points, called the Voronoi points, adopted to construct the Voronoi polygons, are the centroid of the stone that constitutes the sectional morphology of the rubble masonry [Torres and Castaño, 2007].

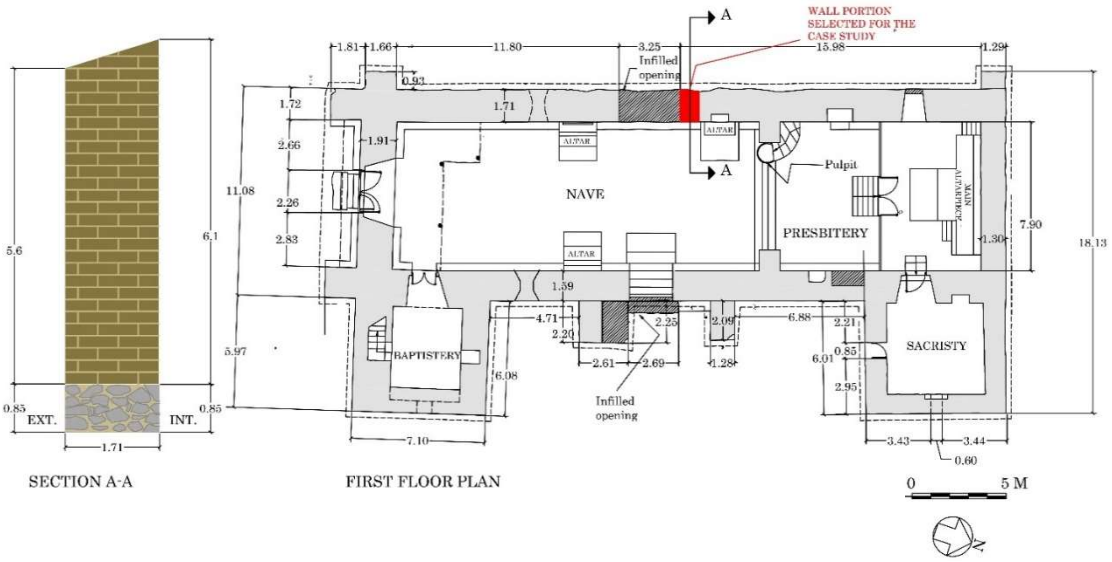

FIGURE 7 Geometry of the west longitudinal wall. (Dimensions in meters)

Two DEM models of the wall were prepared assuming different approaches for the blocks, namely: (a) Model 1, in which the adobe units are deformable and modeled with a Finite Element mesh with edge size of 0.20 m; (b) Model 2, in which the adobe units were modeled as rigid and the faces were triangulated into sub-faces, aiming at increasing the number of contact points and the precision of the results. In both models the stone units of the base course were modeled as rigid blocks, assuming the deformation to occur only at the joints.

The stiffness of the interfaces is represented by two springs in the normal and shear direction, relating the contact stresses with the relative blocks displacements (FIGURE 8) [Lemos, 2007]. When the block is considered as deformable, the normal stiffness of the interfaces (k_n) corresponds to the stiffness of the joint, which is calculated based on the Young's modulus of the joint (E_j) and its thickness (L_j). When the blocks are rigid and the deformability is concentrated at the joints, the normal stiffness of the interfaces (k_n) is calculated as an equivalent stiffness ($k_{n,eq}$), based on the stiffness of one joint and the stiffness of two halves of blocks [Idris et al., 2009; Tran et al., 2014]:

$$\frac{1}{k_{n,eq}} = \frac{2}{k_{n,b}} + \frac{1}{k_{n,j}} \tag{1}$$

where $K_{n,b}$ is the normal stiffness of the block, calculated as a function of the Young's modulus of the block (E_b) and its height ($L_b/2$), and ($K_{n,j}$) is the normal stiffness of the joint, calculated as a function of the Young's modulus of the joint (E_j) and its thickness (L_j). The shear stiffness (k_s) was assumed to be 40% of the normal stiffness (Poisson's ratio equal to 0.25). The non-linear behavior of the mortar assigned to the interfaces corresponds to a Mohr–Coulomb constitutive model, which has the cohesion (c), the friction angle (ϕ) and the tensile strength (f_t) as parameters.

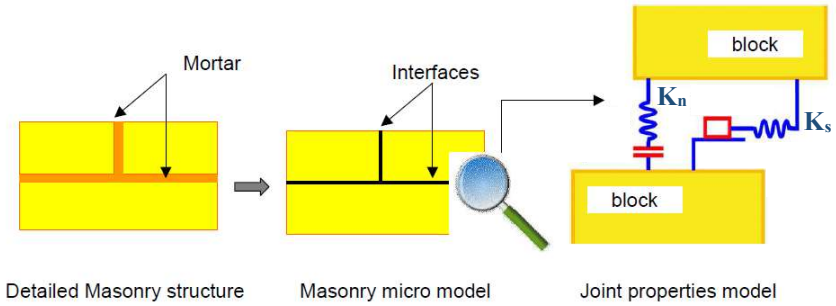

FIGURE 8 Graphic scheme of the interface model (adapted from [Idris et al., 2009]).

The material properties (TABLE 1–3) were defined based on the results of tests carried out by the *Pontificia Universidad Católica del Perú* (PUCP), the in situ sonic tests

performed by University of Minho, and the data available in the literature [Caporale et al., 2015; Greco et al, 2015; IMIT, 2009; Ogburn et al., 2013; Olarte et al., 2013; Silveira et al., 2012; SPR, 2014]. Besides the self-weight of the wall, the vertical and horizontal forces of the self-weight of the roof were applied at the top of the models.

TABLE 1 Elastic properties of Model 1 with deformable blocks.

	Stone units		Adobe units
Density (γ) [kN/m^3]	19*		19*
Young's modulus (E) [MPa]	19400		114
Shear modulus (G) [MPa]	776		46
	Stone–stone interface	Adobe–adobe interface	Adobe–stone interface
Normal stiffness (K_n) [GPa/m]	2.67	5.33	5.33
Shear stiffness (K_s) [GPa/m]	1.07	2.13	2.13

(* The value corresponds to the density of the masonry, taking into account the adopted modeling approach)

TABLE 2 Elastic properties of Model 2 with rigid blocks.

	Stone units		Adobe units
Density (γ) [kN/m^3]	19*		19*
	Stone-stone interface	Adobe–adobe interface	Adobe–stone interface
Normal stiffness (K_n) [GPa/m]	2.60	0.52	0.94
Shear stiffness (K_s) [GPa/m]	1.04	0.21	0.37

(* The value corresponds to the density of the masonry, taking into account the adopted modeling approach)

TABLE 3 Non-linear properties of the interfaces.

	Stone–stone interface	Adobe–adobe interface	Adobe–stone interface
Cohesion (c) [MPa]	0.100	0.044	0.065
Friction angle (ϕ) [º]	22	29	24
Tensile strength (f_t) [MPa]	0.050	0.010	0.010

The evaluation of the out-of-plane behavior of the west longitudinal wall was carried out through a pushover analysis with horizontal forces proportional to the mass. The results of Model 1 (deformable blocks) show that the maximum capacity of the wall equals 0.14 g and 0.23 g for the pushover analysis in the +X direction (outward) and –X direction (inward), respectively (FIGURE 9). As expected, the wall presents a lower load capacity in the +X direction, since the horizontal load of the roof causes a moment favorable to

the collapse of the wall in this direction. Both analyses present collapse mechanisms that correspond to the overturning of the wall with rotation at the base (FIGURE 9). Model 2, with rigid blocks, presents a response similar to that of Model 1 (FIGURE 10). The analysis results show that the difference is about 2% of the maximum horizontal acceleration, with the lowest capacity occurring for Model 1 with rigid blocks. The collapse mechanisms are also similar. However, the cracking at the base seems to be more distributed in Model 1 with deformable blocks (FIGURE 10). It is noted that in Model 2 with rigid blocks the deformability is concentrated at the joints.

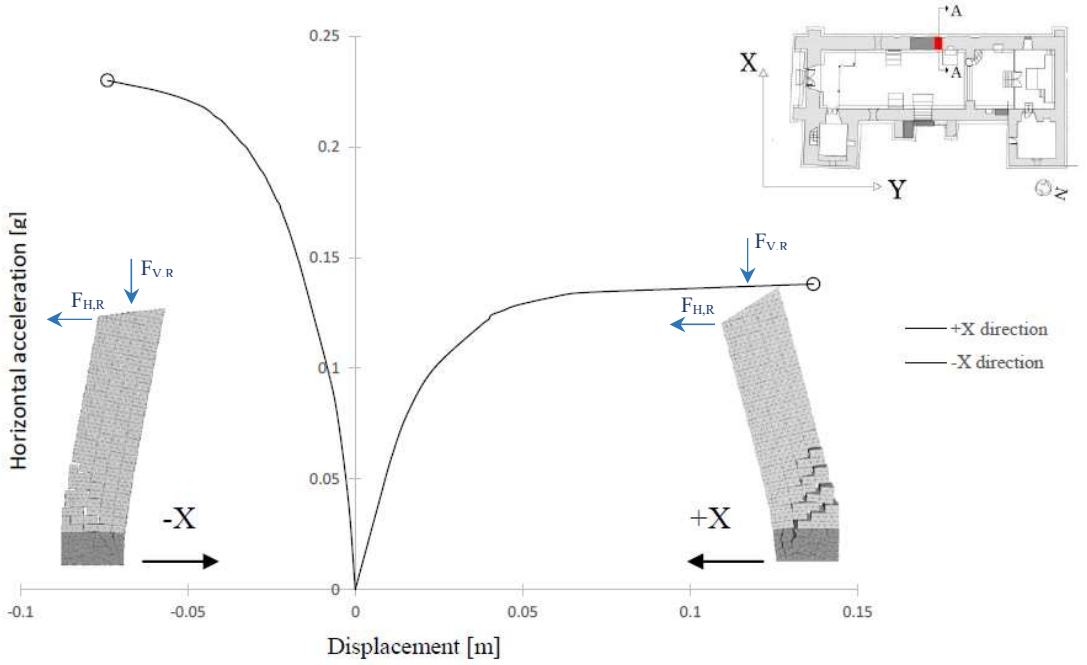

FIGURE 9 Capacity curves of the out-of-plane behavior of the west wall (Model 1 with deformable blocks). ($F_{V,R}$ and $F_{H,R}$ correspond to the vertical and horizontal components of the self-weight of the roof, respectively)

A sensitivity analysis was also carried out, aiming at evaluating the influence of the uncertainties on the dynamic behavior of the wall [Zanotti, 2015], namely: (a) The morphology of the cross-section of the adobe (three patterns based on the English bond pattern); (b) Mesh for modeling the base course of rubble masonry (regular pattern and Voronoi polygons with a maximum edge size of 0.40 m); (c) Non-linear parameters of the interfaces (adobe–adobe interfaces: $0.84c_0 \leq c \leq 1.50c_0$, $0.9\phi_0 \leq \phi \leq 1.2\phi_0$, with

c_0=0.045 MPa, ϕ_0=29º; stone–stone interfaces: $0.70c_0 \leq c \leq 3.00c_0$, $0.9\phi_0 \leq \phi \leq 1.2\phi_0$, with c_0=0.1 MPa, ϕ_0=22º). The sensitivity analysis was performed assuming the adobe units as rigid blocks. The results of the parametric analysis allowed the conclusion that, in general, the differences in the maximum horizontal acceleration are not significant. The highest variation of the maximum horizontal acceleration is equal to 7% (0.15 g) and occurs for the model in which a regular pattern was assumed for the base course (FIGURE 11). All the analyses present the same type of collapse mechanisms characterized by the overturning of the wall with rotation at the base. Therefore, it can be concluded that the simpler rigid block representation gives a good approximation, provided a sufficient number of contact points is used.

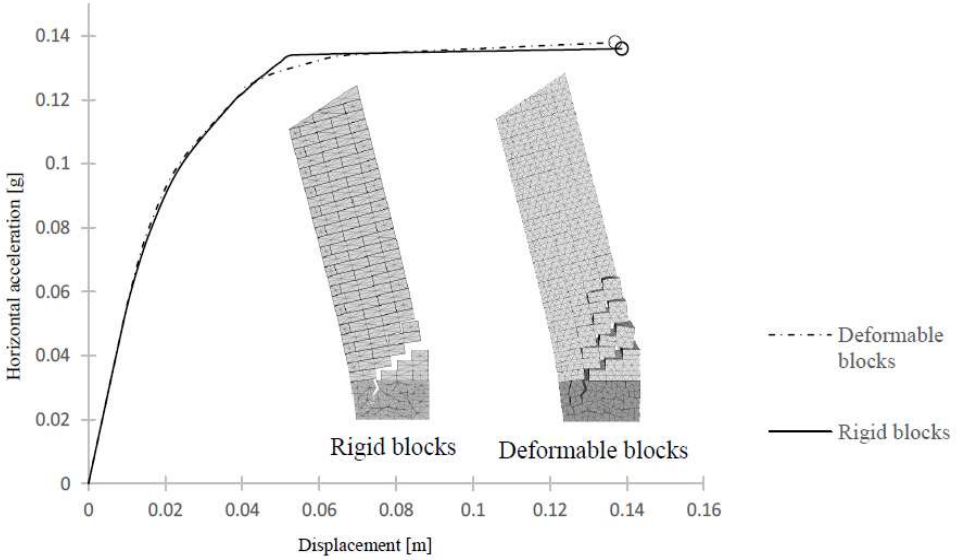

FIGURE 10 Comparison between the capacity curves of the models with deformable (Model 1) and rigid blocks (Model 2).

5. Out-of-plane behavior of the main façade

The main façade presents vertical cracks at the corners (FIGURE 5), showing that it is one of the most vulnerable parts of the Kuño Tambo church. Thus, the out-of-plane response of the main façade, including the connection between the façade and longitudinal walls, was selected for evaluation by means of a partial DEM model of the

church. The DEM model (FIGURE 12) is composed by the main façade and part of the longitudinal walls (about 10 m long). Since the walls of the baptistery do not present an efficient connection to the walls of the nave, the baptistery was not considered in the model of the main façade. The transversal beam existing at the top of the main façade (FIGURE 4) also presents weak connections to the walls and consequently was not considered in the DEM model. The model includes the horizontal timber beams at the lintels of the openings. The self-weight of the roof (vertical and horizontal components) was also taken into account.

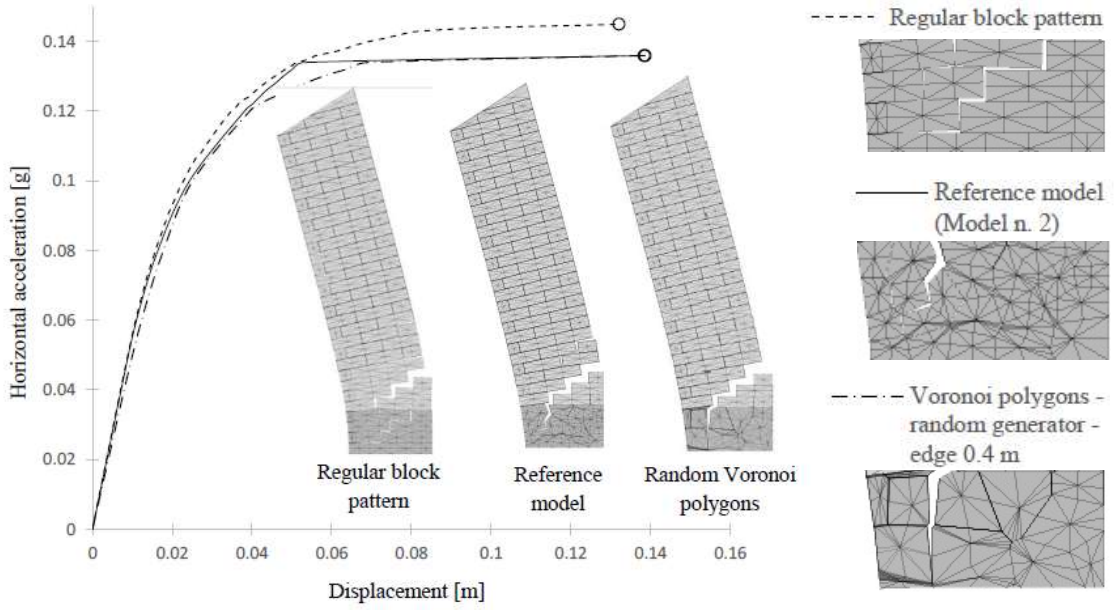

FIGURE 11 Capacity curves of the sensitivity analysis based on different modeling approaches for the rubble stone masonry.

In the DEM model of the main façade, rigid blocks were adopted for both adobe and stone units. The masonry of the base course was modeled by Voronoi polygons with dimensions greater than the real size of the stone units, in order to reduce the computational effort. The initial values of the material properties are the ones adopted for the model of the longitudinal wall (see Section 4), with the exception of the stone–stone and stone–adobe interfaces that take into account the greater dimensions of the blocks adopted for the base course. Furthermore, the modeling methodology was based on the definition of regular

macroblocks that were then discretized into smaller rigid blocks, representative of the adobe units. In this way, the mesh presents vertical joints between the macroblocks. These vertical joints, useful for the model building procedure, were assumed as rigid in order to guarantee the continuity of the blocks, with the exception of the vertical joints at the corners, in which the elastic properties adopted for the joints were assumed.

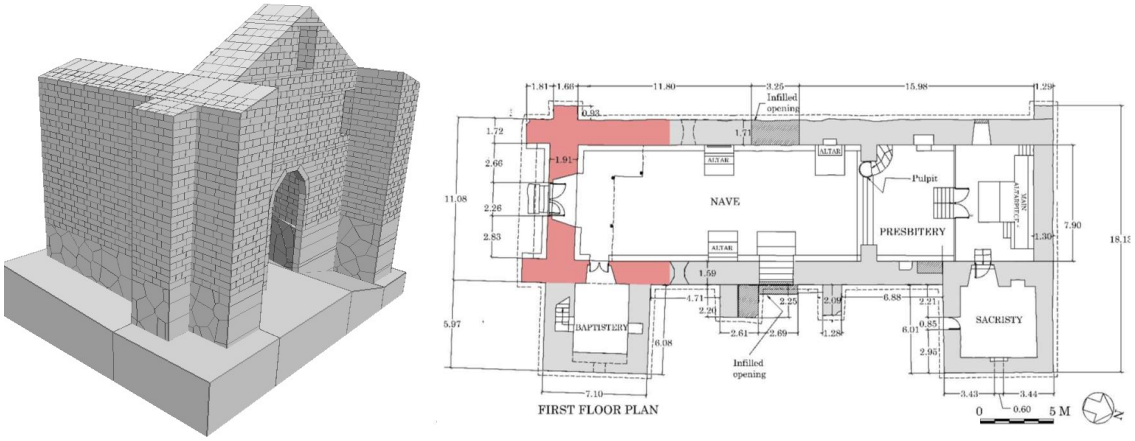

FIGURE 12 Geometry and model of the main façade. (Dimensions in meters)

The façade model was calibrated with respect to the frequency of the first local mode of the main façade (2.15 Hz) estimated in the dynamic identification tests (see Section 3.5), in which the elastic properties of the interfaces were assumed as the variables to be calibrated. The model was calibrated (reference model) through the Douglas–Reid proposal [Douglas and Reid, 1982] and an error of about 3% for the frequency of the first local mode of the main façade was obtained (2.22 Hz). TABLES 4 and 3 present the updated elastic properties and the non-linear properties, respectively.

The corners of the church present overlapping of units at these connections and the behavior of the vertical joints of the model at the corners influences the response of the church. The assumption of adopting the inelastic properties of the unit–mortar interfaces for the vertical interfaces at the corners can underestimate the capacity of the structure. On the other hand, the assumption of simulating the connection between orthogonal walls

as rigid can overestimate the response of the structure. Thus, given the uncertainty about the real condition, the connection between the façade and the longitudinal walls was modeled based on the following hypotheses: (a) Model 1: Inelastic joint with properties of the adobe units (reference model), in which a f_t equal to 0.12 MPa [Silveira et al., 2012], a ϕ equal to 29º and a c equal to 0.18 MPa (c =1.5f_t) were assumed; (b) Model 2: Elastic joint with the same stiffness as mud mortar; (c) Model 3: Joint with very weak connection between orthogonal walls, in which the properties of mud mortar were assumed (f_t = 0.01 MPa, ϕ = 29º and c = 0.044 MPa). For more information on the mechanical properties of adobe based on experimental tests, see [Mahini, 2015] and [Milani and Lourenço, 2013].

TABLE 4 Elastic properties of the main façade model after calibration.

	Stone units	Adobe units	Timber beams
Density (γ) [kN/m^3]	19*	19*	4
	Stone–stone interface	Adobe–adobe interface	Adobe–stone interface
Normal stiffness (K_n) [GPa/m]	1.04	0.40	0.62
Shear stiffness (K_s) [GPa/m]	0.42	0.16	0.25

(* The value corresponds to the density of the masonry, taking into account the adopted modeling approach)

The seismic performance of the main façade was evaluated by means of a pushover analysis with force distribution proportional to the mass in the orthogonal direction to the façade (inward and outward).

The results of the pushover analysis with load applied in the outward direction show that the connection between orthogonal walls has a significant influence on the seismic performance of the main façade (FIGURE 13). The maximum capacity of the model in terms of horizontal acceleration is equal to 0.24 g, 0.34 g (+42%) and 0.15 g (-38%) for Models 1, 2 and 3, respectively. Models 1 and 3 present similar collapse mechanisms, namely the collapse of the façade with a rotation at the base and vertical cracks at the corners (façade wall), which is in agreement with the existing damage (FIGURE 5).

Model 2 presents a collapse mechanism that starts with the collapse of the east wall. This aspect indicates that the connections between orthogonal walls adopted in Model 2 (elastic joints) are significantly more efficient than the existing connections, allowing the transference of inertial forces from the main façade to the longitudinal walls.

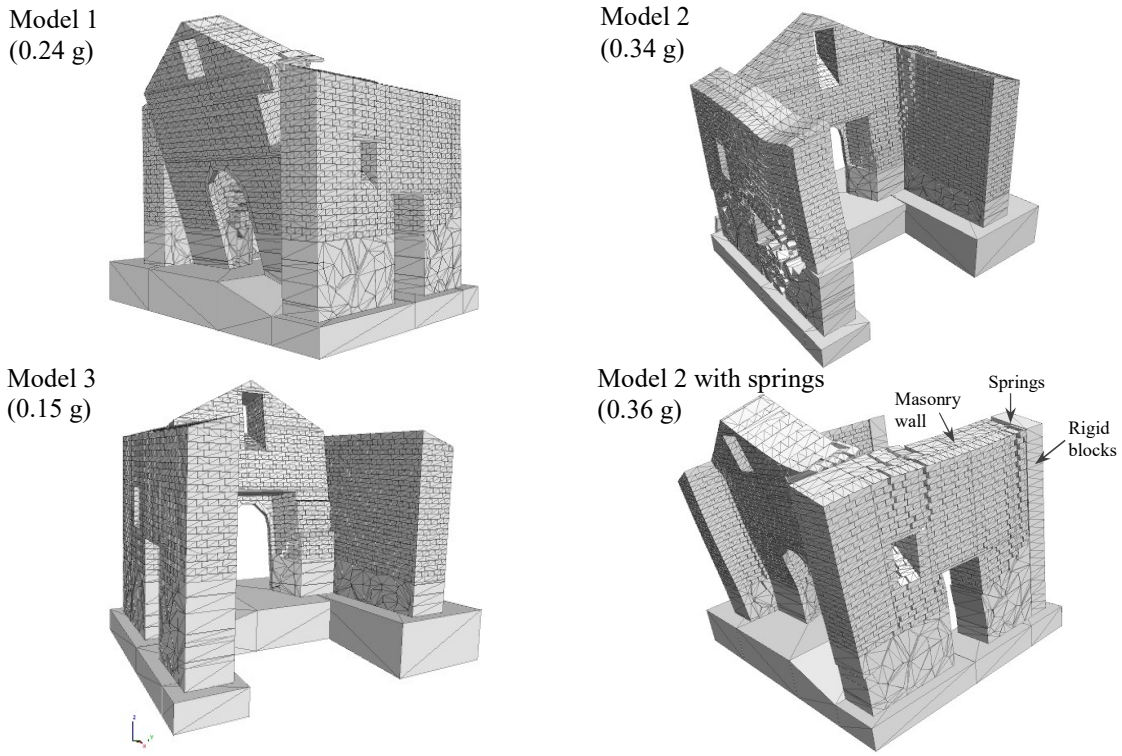

FIGURE 13 Pushover analysis of the main façade in –Y direction (outwards).

The pushover analysis in the inward direction (FIGURE 14) presents the lowest horizontal acceleration of collapse (0.14 g). This value occurs for Model 3 and is associated with the local collapse of the main façade with rotation at the base and vertical cracks at the corners of the façade. Model 1 (reference model) presents a maximum horizontal acceleration equal to 0.19 g (-21% with respect to the pushover in the outward direction). This reduction is associated with the difference of the stiffness and strength of the walls in each direction, namely the ratio between in-plane deformation of the longitudinal walls and the out-of-plane deformation of the main façade in the outward direction. This ratio is higher in the inward direction and the damage is concentrated

mainly at the corners of the main façade (local collapse of the façade with rotation at the base as a rigid body). Model 2 presents a maximum capacity (0.37 g) similar to its capacity in the outward direction (0.34 g).

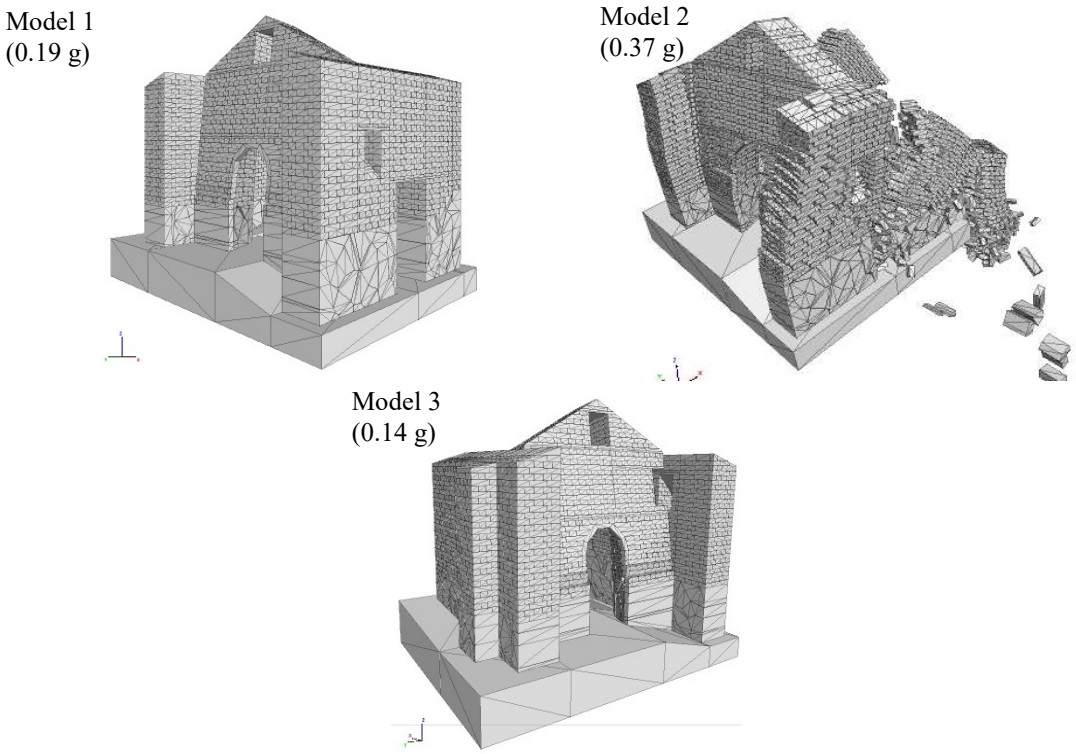

FIGURE 14 Pushover analysis of the main façade in +Y direction (inwards).

Finally, since only a part of the longitudinal walls was considered (about 10 m long), the influence of the in-plane stiffness of these walls on the seismic performance of the main façade was investigated with a DEM model with horizontal springs at the end of the longitudinal walls (FIGURE 13). The springs are intended to include the additional in-plane stiffness of the longitudinal walls not considered in the partial model of the main façade. Only the normal stiffness was considered ($k_{n,spring} = E/L_{wall}$). Model 2, with connections between orthogonal walls able to transfer inertial forces from the façade to the longitudinal wall, was adopted, and a pushover analysis in the outward direction was carried out (lowest load capacity for the Model 2). The results show that Model 2 with springs presents an increase of the maximum load capacity of about 6% with respect to

the model without springs and 50% with respect to the reference model (Model 1). In terms of damage, the collapse mechanism corresponds to the collapse of the main façade involving also part of the orthogonal walls (efficient connections at the corners).

Conclusions

This paper presents the application of DEM for assessing the seismic performance of an adobe church with thick walls (Kuño Tambo church, Peru), in which the morphology of the cross-section can influence the response. The masonry walls are composed by adobe units and mud mortar, built over a base course made of rubble masonry.

Two main models were prepared, aiming at evaluating the out-of-plane response of the west longitudinal wall of the nave without buttresses (2D analysis) and the out-of-plane behavior of the main façade (3D analysis), based on a pushover analysis. The adobe masonry was modeled using a regular pattern with blocks and zero thickness joints, based on the real dimensions of the units. The irregular masonry of the base course was simulated by Voronoi polygons.

In the evaluation of the out-of-plane behavior of the west longitudinal wall, the options of adopting rigid or deformable blocks for the units were also compared. Furthermore, a sensitivity analysis was carried out, in which different patterns for the morphology of the cross-section of the adobe, different patterns for the mesh of the base course, and different values of the non-linear parameters were considered. The results showed that the lowest capacity of the wall is equal to 0.14 g (model with rigid blocks in the outward direction). The collapse of the wall is characterized by its overturning with rotation at the base and diagonal cracks. The model with deformable blocks did not present significant differences, displaying an increase of about 2% of the maximum horizontal acceleration. The results of the sensitivity analysis allowed the conclusion that the pattern of the mesh

of the base course has the greatest influence on the response of the wall (increase of about 7% for the regular pattern of the base course).

The seismic evaluation of the out-of-plane response of the main façade involved the preparation of a 3D DEM model with 6886 rigid blocks. The behavior of the connections between orthogonal walls was also examined, by comparing three assumptions for the corners: (a) Connection with inelastic joint with adobe properties (reference model and calibrated); (b) Connection with elastic joint; (c) Very weak connection. The results indicated that the maximum capacity of the reference model is equal to 0.24 g and 0.19 g, for the pushover analysis in the outward and inward direction, respectively. The collapse mechanism corresponds to the local collapse of the main façade with a rotation at the base and vertical cracks at the corners, which is in agreement with the existing damage to the church. Furthermore, it is concluded that the behavior of the connections between orthogonal walls has a high influence on the response of the structure (-38% to +50% in the outward direction; -26% to +95% in the inward direction). The model with very weak connection displays a concentration of damage at the corners and the response is similar to the response of the model of the wall.

Finally, the results obtained from this numerical work support a proposal of interventions to reduce the seismic vulnerability of the Kuño Tambo church, which includes repairing the existing damage (mainly the cracks at the main façade), reconstructing the collapsed buttresses, strengthening the existing buttresses, and improving the connections between orthogonal walls.

List of symbols

k_n	Normal stiffness
$k_{n,eq}$	Equivalent normal stiffness
k_s	Shear stiffness
$K_{n,j}$	Normal stiffness of the joint
$K_{n,b}$	Normal stiffness of the block
$k_{n,spring}$	Normal stiffness of the springs (Model 2)
E_j	Young's modulus of the joint
L_j	Thickness of the joint
E_b	Young's modulus of the block
L_b	Height of the block
L_{wall}	Length of the longitudinal walls
γ	Density
E	Young's modulus
G	Shear modulus
c	Cohesion
ϕ	Friction angle
f_t	Tensile strength
$F_{V,R}$	Vertical component of the roof self-weight
$F_{H,R}$	Horizontal component of the roof self-weight

Acknowledgments

The authors are grateful to The Getty Research Institute for sharing the data on the Kuño Tambo church and to Itasca Consulting Group for providing the 3DEC software through the IEP Programme.

References

Azevedo, J., Sincraian, G. and Lemos, J. V. [2000] "Seismic behavior of blocky masonry structures," Earthquake Spectra 16 (2), 337–65. doi:http://dx.doi.org/10.1193/1.1586116.

Cancino, C., Lardinois, S., D'Ayala, D., Ferreira, C., Torrealva, D., Meléndez, E. and Santamato, L. [2012] Seismic Retrofitting Project: Assessment of Prototype Buildings, Volume 1, Getty Conservation Institute, Los Angeles, US.

Caporale, A., Parisi, F, Asprone, D., Luciano, R. and Prota, A. [2015] "Comparative micromechanical assessment of adobe and clay brick masonry assemblages based on experimental data sets," Composite Structures 120, 208-220.

Chácara, C., Mendes, N. and Lourenço, P. B. [2017] "Simulation of shake table tests on out-of-plane masonry buildings. Part (IV): Macro and micro FEM based approaches," International Journal of Architectural Heritage 11(1), 103-116. doi:10.1080/15583058.2016.1238972

De Felice, G. [2011] "Out-of-plane seismic capacity of masonry depending on wall section morphology," International Journal of Architectural Heritage, 5(4-5), 466-482. doi:10.1080/15583058.2010.530339

Douglas, B. and Reid, W. [1982] "Dynamic tests and system identification of bridges," Journal of the Structural Division 108(10), 2295-2312.

Ferreira, C. F. and D'Ayala, D. [2012] "Seismic assessment and retrofitting of Peruvian earthen churches by means of numerical modelling," Proc. of the 15th World Conference on Earthquake Engineering, Lisbon, Portugal.

Greco, F., Karanikoloudis, G., Mendes, N. and Lourenço, P. B. [2015] Experimental in situ testing campaign on adobe historic structures in Peru, within the Getty SR Project. Technical report 2015-DEC/E-30

Heyman, J. [1969] "The safety of masonry arches," International Journal of Mechanical Sciences 11 (4), 363–85. doi:10.1016/0020-7403(69)90070-8.

Idris, J., Al Heib, M. and Verdel, T. [2009] “Masonry joints mechanical behaviour evolution in built tunnels. Analysis by numerical modelling and experimental design,” Tunnelling and Underground Space Technology 24(6), 617–626.

IMIT [2009] Circ. 02.02.2009, n. 617: Istruzioni per l’applicazione delle Nuove Norme Tecniche per le Costruzioni di cui al decreto ministeriale 14 gennaio 2008. Italian Ministry of Infrastructures and Transportation, Rome, Italy.

ITASCA [2015] 3DEC – Distinct Element Modeling of jointed and blocky material in 3D, ITASCA Consulting Group, Inc, Minneapolis, MN.

Karanikoloudis, G. and Lourenço, P. B. [2015] Seismic Assessment of Kuño Tambo Church (Current Condition), Peru. Technical report 2015-DEC/E- 41.

Lagomarsino, S., Penna, A., Galasco, A. and Cattari, S. [2012] TREMURI program: Seismic Analyses of 3D Masonry Buildings, Italy, University of Genoa.

Lemos, J. V. [2007] “Discrete element modeling of masonry structures,” International Journal of Architectural Heritage 1(2), 190-213. doi: 10.1080/15583050601176868

Lemos, J. V. [2016] “The basis for masonry analysis with UDEC and 3DEC,” in Computational Modeling of Masonry Structures Using the Discrete Element Method, eds. V. Sarhosis, K. Bagi, J. V. Lemos and G. Milani (IGI Global), pp. 61-89. doi:10.4018/978-1-5225-0231-9.ch003

Lemos, J. V. and Costa, A. C. [2017] “Simulation of shake table tests on out-of-plane masonry buildings. Part (V): Discrete element approach,” International Journal of Architectural Heritage 11(1), 117-124. doi:10.1080/15583058.2016.1237587

Lourenço, P. B. [2002] “Computations on historic masonry structures,” Structural Engineering and Materials 4 (3), 301–19. doi:10.1002/pse.120.

Lourenço, P. B., Mendes, N., Ramos, L. F. and Oliveira, D. V. [2011] "Analysis of masonry structures without box behavior," International Journal of Architectural Heritage 5 (4–5), 369-82. doi:10.1080/15583058.2010.528824.

Magenes, G. and Fontana, A. [1998] "Simplified non-linear seismic analysis of masonry buildings," Proc. of the British Masonry Society, No. 8.

Mahini, S. [2015] "Smeared crack material modelling for the nonlinear analysis of CFRP-retrofitted historical brick vaults with adobe piers," Construction & Building Materials 74, 201-218. doi:10.1016/j.conbuildmat. 2014.10.033).

McInerney, J. and DeJong M. J. [2015] "Discrete element modeling of groin vault displacement capacity," International Journal of Architectural Heritage 9(8), 1037-1049, doi:10.1080/15583058.2014.923953

Milani, G. and Lourenço, P. B. [2013] "Simple homogenized model for the nonlinear analysis of FRP-strengthened masonry structures. II: Structural applications," Journal of Engineering Mechanics 139(1), 77-93.

Mendes, N. and Lourenço P. B. [2010] "Seismic assessment of masonry "Gaioleiro" buildings in Lisbon, Portugal," Journal of Earthquake Engineering 14(1), 80-101. doi: 10.1080/13632460902977474.

Mendes, N. and Lourenço, P. B. [2014] "Sensitivity analysis of the seismic performance of existing masonry buildings," Engineering Structures 80(1), 137–46. doi:10.1016/j.engstruct.2014.09.005.

Mendes, N., Costa, A. A., Lourenço, P. B., Bento, R., Beyer, K., Felice, G., Gams, M., Griffith, M., Ingham, J., Lagomarsino, S., Lemos, J. V., Liberatore, D., Modena, C., Oliveira, D. V., Penna, A. and Luigi Sorrentino, L. [2017] "Methods and approaches for blind test predictions of out-of-plane behavior of masonry walls: A numerical

comparative study," International Journal of Architectural Heritage 11(1), pp 59-71. http://dx.doi.org/10.1080/15583058.2016.1238974

Mumford, J. R. [2012] Vertical Empire: The General Resettlement of Indians in the Colonial Andes. Duke University Press, Durham, NC.

Ogburn, D., Sillar, B. and Sierra, J. C. [2013] "Evaluating effects of chemical weathering and surface contamination on the in situ provenance analysis of building stones in the Cuzco region of Perù with portable XRF," Journal of Archeological Science 40(4), 1823-1837.

Olarte, J., Proaño, R., Scaletti, H., Torres, M. and Zavala, C. [2013] Evaluaciòn de la vulnerabilidad sìsmica de la Catedral del Cusco, Universidad Nacional de Ingegnerìa, Facultad de Ingegnerìa Civil, Peru.

Peña, F., Lourenço, P. B., Mendes, N. and Oliveira, D. V. [2010] "Numerical models for the seismic assessment of an old masonry tower," Engineering Structures 32(5), 1466–78. doi:10.1016/j.engstruct.2010.01.027.

Psycharis, I. N., Lemos, J. V., Papastamatiou, D. Y., Zambas, C. and Papantonopoulos, C. [2003] "Numerical study of the seismic behaviour of a part of the Parthenon Pronaos," Earthquake Engineering and Structural Dynamics 32(13), 2063-2084. doi:10.1002/eqe.315

Psycharis, I. N., Drougas, A. and Daisou, M. [2011] "Seismic behaviour of the walls of the Parthenon: A Numerical Study," Computational Methods in Earthquake Engineering. Computational Methods in Applied Sciences 21, 265-283. doi:10.1007/978-94-007-0053-6_12

Roca, P., Cervera, M., Gariup, G. and Pela, L. [2010] "Structural analysis of masonry historical constructions. Classical and advanced approaches," Archives of Computational Methods in Engineering 17(3), pp 299-325. doi: 10.1007/s11831-010-9046-1

Silveira, D., Varum, H., Costa, A., Martins, T., Pereira, H. and Almeida, J. [2012] "Mechanical properties of adobe bricks in ancient constructions," Construction and Building Materials 28(1), 36–44.

SPR [2014] Seismic Retrofitting Project: Testing and Modelling, Chapter 3, Getty Conservation Institute and Pontificia Universidad Católica del Perú.

Torres, S. A. G. and Castaño J. D. M. [2007] "Simulation of the hydraulic fracture process in two dimensions using a discrete element method," Physical Review E 75(6), 066109.

Tran, V. H., Vincens, E., Morel, J.C., Dedecker, F. and Le, H. H. [2014] "2D-DEM modeling of the formwork removal of a rubble stone masonry bridge," Engineering Structures 75, 448-456.

Young, M. P. Schultz, A. E. and Lemos, J. V. [2015] "Seismic analysis of the Panhellenic Sanctuary of Nemea, Greece," Proc. of the 12th North American Masonry Conference.

Zanotti, S. [2015] Seismic analysis of the church of Kuño Tambo, Master's Thesis, Advanced Masters in Structural Analysis of Monuments and Historical Constructions, University of Minho, Guimarães, Portugal.